Magnetic Resonance Imaging 35 (2015) 1178–1181

Contents lists available at ScienceDirect

Magnetic Resonance Imaging

journal homepage: www.mrijournal.com

Prostate diffusion imaging with distortion correction☆

Rebecca A. Rakow-Penner [a], Nathan S. White [a], Daniel J.A. Margolis [b], John Kellogg Parsons [c], Natalie Schenker-Ahmed [a], Joshua M. Kuperman [a], Hauke Bartsch [a], Hyung W. Choi [a], William G. Bradley [a], Ahmed Shabaik [d], Jiaoti Huang [e], Michael A. Liss [f], Leonard Marks [g], Christopher J. Kane [c], Robert E. Reiter [g], Steven S. Raman [b], David S. Karow [a,*], Anders M. Dale [a]

[a] Department of Radiology, University of California San Diego School of Medicine
[b] Department of Radiology, University of California Los Angeles Geffen School of Medicine
[c] Department of Urology, University of California San Diego School of Medicine
[d] Department of Pathology, University of California San Diego School of Medicine
[e] Department of Pathology, University of California Los Angeles Geffen School of Medicine
[f] Department of Urology, University of Texas Health Science Center San Antonio
[g] Department of Urology, University of California Los Angeles Geffen School of Medicine

ARTICLE INFO

Article history:
Received 3 February 2015
Revised 9 July 2015
Accepted 19 July 2015

Keywords:
Prostate cancer
MRI
Diffusion-weighted imaging
Distortion correction

ABSTRACT

Purpose: Diffusion imaging in the prostate is susceptible to distortion from B0 inhomogeneity. Distortion correction in prostate imaging is not routinely performed, resulting in diffusion images without accurate localization of tumors. We performed and evaluated distortion correction for diffusion imaging in the prostate.

Materials and methods: 28 patients underwent pre-operative MRI (T2, Gadolinium perfusion, diffusion at b = 800 s/mm^2). The restriction spectrum protocol parameters included b-values of 0, 800, 1500, and 4000 s/mm^2 in 30 directions for each nonzero b-value. To correct for distortion, forward and reverse trajectories were collected at b = 0 s/mm^2. Distortion maps were generated to reflect the offset of the collected data versus the corrected data. Whole-mount histology was available for correlation.

Results: Across the 27 patients evaluated (excluding one patient due to data collection error), the average root mean square distortion distance of the prostate was 3.1 mm (standard deviation, 2.2 mm; and maximum distortion, 12 mm).

Conclusion: Improved localization of prostate cancer by MRI will allow better surgical planning, targeted biopsies and image-guided treatment therapies. Distortion distances of up to 12 mm due to standard diffusion imaging may grossly misdirect treatment decisions. Distortion correction for diffusion imaging in the prostate improves tumor localization.

1. Introduction

In the United States, prostate cancer is the leading cause of cancer in men and the second leading cause of cancer deaths [1]. Multiparametric magnetic resonance imaging (MRI) plays a large role in staging and localizing prostate cancer, with diffusion imaging as a key component [2–16]. Diffusion imaging often increases the conspicuity of prostate cancers and detects them with greater accuracy than T2 or perfusion imaging [5,8,9]. However, standard diffusion sequences with echo planar imaging (EPI) for k-space sampling suffer from distortion artifacts due to B0 inhomogeneity [17,18]. These distortion artifacts obscure the precise location of concerning findings with this technique. Improved tumor localization with diffusion imaging would enhance MRI's utility in evaluating prostate cancer. Surgical management of prostate cancer often depends on a priori knowledge of tumor extension beyond the prostatic capsule, determining nerve-sparing techniques versus aggressive surgery. In addition, novel techniques and treatments such as MRI-Ultrasound fusion guided biopsies [19] and high-intensity focused ultrasound treatment [20,21], depend on accurate localization of prostate cancer, where a subset may only be detected with diffusion MRI.

Routine standard of care diffusion with EPI does not incorporate correction for B0 inhomogeneity distortions. Techniques for distortion correction for diffusion imaging with EPI exist [22–24] and have been applied in the brain [23,24].

☆ No conflicts of interests.

* Corresponding author at: Multimodal Imaging Laboratory, 8950 Villa La Jolla Drive Suite C101, La Jolla, CA 92037. Tel./fax: +1 858 534 1078.
E-mail address: dskarow@ucsd.edu (D.S. Karow).

http://dx.doi.org/10.1016/j.mri.2015.07.006
0730-725X/

Table 1
MRI scan parameters.

Pulse sequence	Parameters
T2	Axial 3D TSE T2 (Siemens SPACE) TR/TE 3800–5040/101 ETL 13, 14 cm FOV, 256 × 256 matrix, 1.5 mm contiguous slices, 60 slices
Diffusion-weighted (Standard)	Echoplanar, TR/TE 3900/60, 21 × 26 cm FOV, 130 × 160 matrix, 3.6 mm slices, 4 NEX, b-values of 0, 100, 400, and 800 s/mm^2, 20 slices, parallel imaging with a factor of 2
T1 Dynamic Perfusion Imaging	Siemens TWIST, TR./TE 3.9/1.4 ms, 12° flip angle, 26 × 26 cm FOV, 160 × 160 matrix, 3.6 mm slices, 4.75 s/acquisition over 6 min with 15 s injection delay, image analysis using iCAD Versavue,
Restriction Spectrum Imaging	Spin echo EPI, TR/TE 5500/137, 26 × 26 cm FOV, 128 × 96 matrix, 3.6 mm slices, 30 directions at each b-value, b-values of 0, 800, 1500, and 4000 s/mm^2, 60 slices

In this paper, a diffusion MRI technique called Restriction Spectrum Imaging (RSI-MRI) [25–28] was used to evaluate 28 preoperative prostate cancer patients and assess the benefits of correcting for B0 distortion effects. This study is a further evaluation of data used in our initial proof of concept study of RSI-MRI of the prostate [28]. RSI-MRI incorporates distortion correction [23] as part of its image post-processing stream.

2. Materials and methods

Preoperative MRI was performed on 28 prostate cancer patients in this IRB approved study. The patients underwent the standard multi-parametric prostate MRI protocol using 3 T MRI systems (TrioTim, Skyra, Siemens, Erlangen, Germany) with an endorectal coil (Medrad, Warrendale, PA) (Table 1): T2 weighted-MRI, dynamic contrast-enhanced (DCE) MRI with gadolinium-based contrast agent, and diffusion-weighted MRI (b = 800 s/mm^2). In addition, the diffusion protocol included b values of 0, 800, 1500, and 4000 s/mm^2 in 30 unique diffusion directions for each nonzero b-value. The distortion-correction algorithm [23] utilizes the symmetry of the distortion from B0 inhomogeneity (Fig. 1). By collecting images at b = 0 s/mm^2 in both the forward and reverse phase encode trajectories, a deformation field map can be calculated and used to correct the entire diffusion data set. For one patient out of the 28 patients, there was an error in the scan parameters for the forward and reverse images, and thus distortion correction could not be performed. This patient was excluded from the evaluation, leaving 27 patients for analysis.

RSI-MRI cellularity maps were reconstructed based on all b-values [25], distortion corrected and then standardized across the sample with z-score maps. The z-score maps were calculated by (1) measuring the mean and standard deviation of normal prostate signal from the raw cellularity maps across the patient pool, (2) subtracting this measured mean value from each subject's cellularity map, and (3) dividing by the measured normal prostate standard deviation. Distortion maps were also generated to reflect the offset of the collected data in the phase encode direction versus the distortion corrected data. In addition to multi b-value cellularity maps, a low b-value ADC (b = 800 s/mm^2) map was also generated and distortion-corrected. Whole-mount histopathology was available for correlation. With whole-mount histopathology, the tumor area was identified by an experienced uropathologist.

With the T2 weighted-image, a radiologist delineated a region of interest determined by the prostatic capsule. The region of interest was overlaid on the distortion correction map to measure the mean and standard deviation of the distortion correction in the phase encode direction. This information was used to calculate the root mean square (RMS) distortion distance for the entire prostate in a single slice according to the following relationship:

$$RMS_{distortion} = 2 \times \sqrt{\left(\mu_{distortion\ distance}{}^2 + \sigma_{distortion\ distance}{}^2\right)}$$

where $\mu_{distortion\ distance}$ is the mean distortion distance and $\sigma_{distortion\ distance}$ is the standard deviation of the distortion distance measured on the distortion maps.

Low b-value ADC maps (b = 800 s/mm^2) were used to define malignant regions of interest, corresponding to tumors identified on whole mount pathology. In some patients, two regions of interest corresponded to tumor. If on the same slice, both of these tumor regions of interest were included in the analysis, for a total of 34 tumor regions of interest in 27 prostates.

Table 2
Distortion distance of the whole prostate and tumor regions of interest due to B0 inhomogeneity.

	Mean (standard deviation) (mm)	Maximum distortion (mm)
Whole prostate distortion	3.2 (2.2)	12
Tumor ROI distortion	3.2 (2.4)	13

3. Results

Across the 27 included patients, the average root mean square distortion distance of the prostate was 3.1 mm (standard deviation, 2.2 mm; maximum distortion, 12 mm). When specifically looking at the tumor regions, the average root mean square of the distortion distance of the tumors was similar at 3.1 mm (standard deviation, 2.3 mm; maximum distortion, 13 mm). Results are summarized in Table 2.

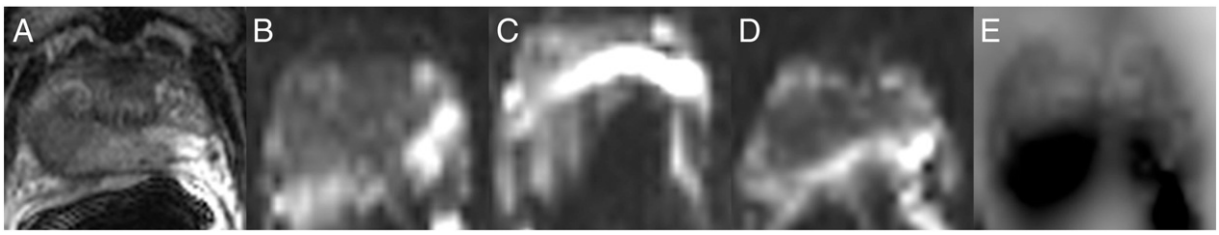

Fig. 1. Demonstration of distortion of diffusion MRI with EPI due to B0 inhomogeneity. (A) T2-weighted image of the prostate reflecting the prostate's MR anatomical appearance without distortion. (B) Demonstration of the distortion when the diffusion data are collected only in the forward phase encode direction with an EPI trajectory. (C) Demonstration of the distortion when the diffusion data are collected only in the reverse phase encode direction with an EPI trajectory. (D) Distortion corrected diffusion imaging at b = 0. (E) Deformation field map.

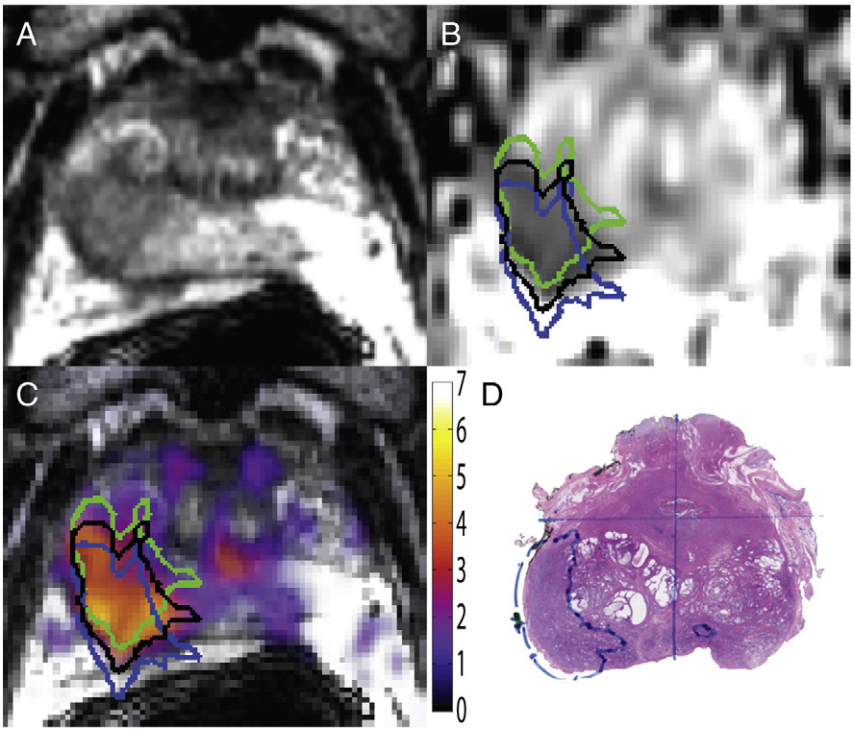

Fig. 2. Patient example of the effects of distortion on localizing tumor. (A) T2-weighted image, used as the imaging anatomic gold standard. Note that the tumor is in the right posterior quadrant. (B) Distortion-corrected low b-value ADC map, with the region of low ADC outlined in black. The blue and green ROIs represent the regions of low ADC without distortion correction (blue: in-phase encode direction, green: reverse phase encode direction). (C) RSI-MRI image that incorporates the distortion correction and converts the cellularity map based on multiple b-values to a standardized z-score map, overlaid on the T2-weighted anatomic image. The blue and green ROIs are the regions of RSI signal without distortion correction while the black ROI is distortion corrected. (D) Whole-mount histopathology confirming the location of extraprostatic extension in the right posterior quadrant.

Nine of the 27 patients demonstrated histologically proven extracapsular extension. Standard diffusion MR of the prostate only identified one tumor as definitively demonstrating extracapsular extension. The distortion correction maps demonstrated extracapsular extension in eight of the nine patients.

Fig. 2 shows an example of the calculated offset by 5.5 mm of root mean square distortion. This patient has histologically proven extraprostatic extension. Depending on the phase encode direction, the tumor area may incorrectly be localized anteriorly (thus not identifying extraprostatic extension), or appear to exceed the prostatic capsule in excess.

4. Discussion

Diffusion imaging, because it uses an echo planar trajectory, is sensitive to B0 inhomogeneity. This manifests as distortion in the phase encode direction. By collecting data in both the forward and reverse phase encoding directions at $b = 0$, enough information is collected to correct for the distortion in the phase encode direction. This technique [23] is used to correct for distortion in brain diffusion imaging. Although diffusion imaging in the prostate is becoming the standard of care in prostate MRI protocols, distortion correction has not yet been widely implemented for prostate diffusion imaging. Other distortion minimizing techniques are being evaluated in the prostate but focus on minimizing the distortion rather than correcting for distortion due to B0 inhomogeneity [29,30].

As demonstrated in this paper, distortion correction improves tumor localization for diffusion imaging. Diffusion imaging is often the best MR technique to detect prostate cancer. With the advent of MRI-ultrasound fusion guided biopsies [19] and high-intensity focused ultrasound treatment [20,21], accurate localization is necessary. Surgical planning also depends on differentiating between extraprostatic extension of tumor and the tumor remaining within the capsule, a decision that could be made with accurate imaging. Distortion distances of up to 13 mm due to standard diffusion imaging may grossly misdirect treatment decisions and therapies. Distortion correction for diffusion imaging has the potential to improve the standard of care for prostate MRI.

Acknowledgements

The authors would like to thank Brenda Brown for her help on this project. Funding: This work was supported by the Department of Defense, Prostate Cancer Research Program W81XWH-13-1-0391, the American Cancer Society–Institutional Research Grant #70-002, NIH-EB-RO1000790, and UCSD Clinician Scientist Program NIH T32-EB005970.

References

[1] Siegel R, Ma J, Zou Z, Jemal A. Cancer statistics. 2014;64:9–29.
[2] Mazaheri Y, Hricak H, Fine SW, et al. Prostate tumor volume measurement with combined T2-weighted imaging and diffusion-weighted MR: correlation with pathologic tumor volume. Radiology 2009;252:449–57. http://dx.doi.org/10.1148/radiol.2523081423.
[3] Tanimoto A, Nakashima J, Kohno H, Shinmoto H, Kuribayashi S. Prostate cancer screening: the clinical value of diffusion-weighted imaging and dynamic MR imaging in combination with T2-weighted imaging. J Magn Reson Imaging 2007;25:146–52. http://dx.doi.org/10.1002/jmri.20793.
[4] Rais-Bahrami S, Siddiqui MM, Turkbey B, et al. Utility of multiparametric magnetic resonance imaging suspicion levels for detecting prostate cancer. J Urol 2013;190:1721–7. http://dx.doi.org/10.1016/j.juro.2013.05.052.
[5] Miao H, Fukatsu H, Ishigaki T. Prostate cancer detection with 3-T MRI: comparison of diffusion-weighted and T2-weighted imaging. Eur J Radiol 2007;61:297–302. http://dx.doi.org/10.1016/j.ejrad.2006.10.002.
[6] Haider MA, van der Kwast TH, Tanguay J, Evans AJ, Hashmi A-T, Lockwood G, et al. Combined T2-weighted and diffusion-weighted MRI for localization of

prostate cancer. AJR Am J Roentgenol 2007;189:323–8. http://dx.doi.org/10.2214/AJR.07.2211.
[7] Donati OF, Jung SI, Vargas HA, Gultekin DH, Zheng J, Moskowitz CS, et al. Multiparametric prostate MR imaging with T2-weighted, diffusion-weighted, and dynamic contrast-enhanced sequences: are all pulse sequences necessary to detect locally recurrent prostate cancer after radiation therapy? Radiology 2013;268:440–50. http://dx.doi.org/10.1148/radiol.13122149.
[8] Lim HK, Kim JK, Kim KA, Cho K-S. Prostate cancer: apparent diffusion coefficient map with T2-weighted images for detection—a multireader study. Radiology 2009;250:145–51. http://dx.doi.org/10.1148/radiol.2501080207.
[9] Isebaert S, Van den Bergh L, Haustermans K, et al. Multiparametric MRI for prostate cancer localization in correlation to whole-mount histopathology. J Magn Reson Imaging 2013;37:1392–401. http://dx.doi.org/10.1002/jmri.23938.
[10] Rastinehad AR, Baccala AA, Chung PH, et al. D'Amico risk stratification correlates with degree of suspicion of prostate cancer on multiparametric magnetic resonance imaging. J Urol 2011;185:815–20. http://dx.doi.org/10.1016/j.juro.2010.10.076.
[11] Rais-Bahrami S, Türkbey B, Rastinehad AR, et al. Natural history of small index lesions suspicious for prostate cancer on multiparametric MRI: recommendations for interval imaging follow-up. Diagn Interv Radiol 2014. http://dx.doi.org/10.5152/dir.2014.13319.
[12] Abd-Alazeez M, Kirkham A, Ahmed HU, Arya M, Anastasiadis E, Charman SC, et al. Performance of multiparametric MRI in men at risk of prostate cancer before the first biopsy: a paired validating cohort study using template prostate mapping biopsies as the reference standard. Prostate Cancer Prostatic Dis 2014;17:40–6. http://dx.doi.org/10.1038/pcan.2013.43.
[13] Hoeks CMA, Somford DM, van Oort IM, et al. Value of 3-T multiparametric magnetic resonance imaging and magnetic resonance-guided biopsy for early risk restratification in active surveillance of low-risk prostate cancer: a prospective multicenter cohort study. Investig Radiol 2014;49:165–72. http://dx.doi.org/10.1097/RLI.0000000000000008.
[14] Stamatakis L, Siddiqui MM, Nix JW, et al. Accuracy of multiparametric magnetic resonance imaging in confirming eligibility for active surveillance for men with prostate cancer. Cancer 2013;119:3359–66. http://dx.doi.org/10.1002/cncr.28216.
[15] Abd-Alazeez M, Ahmed HU, Arya M, Charman SC, Anastasiadis E, Freeman A, et al. The accuracy of multiparametric MRI in men with negative biopsy and elevated PSA level–can it rule out clinically significant prostate cancer? Urol Oncol 2014;32:45.e17–22. http://dx.doi.org/10.1016/j.urolonc.2013.06.007.
[16] Park JJ, Kim CK, Park SY, Park BK, Lee HM, Cho SW. Prostate cancer: role of pretreatment multiparametric 3-T MRI in predicting biochemical recurrence after radical prostatectomy. AJR Am J Roentgenol 2014;202:W459–65. http://dx.doi.org/10.2214/AJR.13.11381.
[17] Le Bihan D, Poupon C, Amadon A, Lethimonnier F. Artifacts and pitfalls in diffusion MRI. J Magn Reson Imaging 2006;24:478–88. http://dx.doi.org/10.1002/jmri.20683.
[18] Donato F, Costa DN, Yuan Q, Rofsky NM, Lenkinski RE, Pedrosa I. Geometric distortion in diffusion-weighted MR imaging of the prostate-contributing factors and strategies for improvement. Acad Radiol 2014;21:817–23. http://dx.doi.org/10.1016/j.acra.2014.02.001.
[19] Pinto PA, Chung PH, Rastinehad AR, et al. Magnetic resonance imaging/ultrasound fusion guided prostate biopsy improves cancer detection following transrectal ultrasound biopsy and correlates with multiparametric magnetic resonance imaging. J Urol 2011;186:1281–5. http://dx.doi.org/10.1016/j.juro.2011.05.078.
[20] Napoli A, Anzidei M, De Nunzio C, Cartocci G, Panebianco V, De Dominicis C, et al. Real-time magnetic resonance-guided high-intensity focused ultrasound focal therapy for localised prostate cancer: preliminary experience. Eur Urol 2013;63:395–8. http://dx.doi.org/10.1016/j.eururo.2012.11.002.
[21] Ahmed HU, Hindley RG, Dickinson L, Freeman A, Kirkham AP, Sahu M, et al. Focal therapy for localised unifocal and multifocal prostate cancer: a prospective development study. Lancet Oncol 2012;13:622–32. http://dx.doi.org/10.1016/S1470-2045(12)70121-3.
[22] Jezzard P, Balaban RS. Correction for geometric distortion in echo planar images from B0 field variations. Magn Reson Med 1995;34:65–73. http://dx.doi.org/10.1002/mrm.1910340111.
[23] Holland D, Kuperman JM, Dale AM. Efficient correction of inhomogeneous static magnetic field-induced distortion in echo planar imaging. Neuroimage 2010;50:175–83. http://dx.doi.org/10.1016/j.neuroimage.2009.11.044.
[24] Andersson JLR, Skare S, Ashburner J. How to correct susceptibility distortions in spin-echo echo-planar images: application to diffusion tensor imaging. Neuroimage 2003;20:870–88. http://dx.doi.org/10.1016/S1053-8119(03)00336-7.
[25] White NS, Leergaard TB, D'Arceuil H, Bjaalie JG, Dale AM. Probing tissue microstructure with restriction spectrum imaging: histological and theoretical validation. Hum Brain Mapp 2013;34:327–46. http://dx.doi.org/10.1002/hbm.21454.
[26] White NS, McDonald CR, Farid N, Kuperman JM, Kesari S, Dale AM. Improved conspicuity and delineation of high-grade primary and metastatic brain tumors using "restriction spectrum imaging": quantitative comparison with high b-value DWI and ADC. AJNR Am J Neuroradiol 2012. http://dx.doi.org/10.3174/ajnr.A3327.
[27] White NS, Dale AM. Distinct effects of nuclear volume fraction and cell diameter on high b-value diffusion MRI contrast in tumors. Magn Reson Med 2013. http://dx.doi.org/10.1002/mrm.25039 [n/a–n/a].
[28] Rakow-Penner R, White N, Parsons JK, Choi H, Liss M, Kuperman J, et al. Novel technique for characterizing prostate cancer utilizing MRI Restriction Spectrum Imaging: proof of principle and initial clinical experience with extra-prostatic extension. Prostate Cancer Prostatic Dis 2015;18:81–5. http://dx.doi.org/10.1038/pcan.2014.50.
[29] Thierfelder KM, Scherr MK, Notohamiprodjo M, Weib J, Dietrich O, Mueller-Lisse UG, et al. Diffusion-weighted MRI of the prostate: advantages of zoomed EPI with parallel-transmit-accelerated 2D-selective excitation imaging. Eur Radiol 2014;24:3233–41. http://dx.doi.org/10.1007/s0030-014-3347-y.
[30] Rosenkrantz AB, Chandarana H, Pfeuffer J, Triolo M, Shaikh MB, Mossa DJ, et al. Zoomed echo-planar imaging using parallel transmission: impact on image quality of diffusion-weighted imaging of the prostate at 3 T. Abdom Imaging 2015;40:120–6. http://dx.doi.org/10.1007/s00261-014-0181-2.